SEMI-AUTOMATED KIDNEY MRI SEGMENTATION USING OPTIMAL THRESHOLDING TECHNIQUE (OTT) IN ADAPTIVE NLM FILTERING

S. Prabhu Das[*1], B. N. Jagadeesh[2] and B. Prabhakara Rao[3]

[*1]Department of Electronics and Communication Engineering, JNTUK, Kakinada, INDIA

[2]Department of Computer Science Engineering, SIET, Amalapuram, INDIA;

[3]Department of Electronics and Communication Engineering, JNTUK, Kakinada, INDIA

Abstract:

Biomedical image processing is an important field of medical image in analyzing, and determining the diameter, volume, and vasculature of a tumor or organ. Kidneys are bean-shaped organs that filter blood and excrete waste, maintaining blood pressure as well as eliminating toxins. Segmentation Accuracy plays a vital role in quantifying kidney structure and volume to estimate the kidney disease and also preprocessing is an important stage in segmentation process. Moreover, Clinical methods are not useful to find GFR for single Kidney when compared to imaging techniques. To improve the segmentation accuracy for Kidney MRI images, to quantify the Surface area and Volume of Kidney Compartments to estimate the kidney disease, an adaptive NLM algorithm with new proposed thresholding is adapted to denoising the MRI image and a fast and simple Chan-Vese (CV) levelset formulation used to split the kidney structure from its background. Further, a hard clustering technique used to segment the kidney compartments. The overall performance evaluated in performance metrics such as segmentation Accuracy, Sensitivity, MCC, Dice Coefficient and Jaccard Index. The performance metrics compared with Threshold based FCM. The segmentation results were shown best accuracy nearly 99.7% and very good performance metrics.

Keywords: Abnormalities, Renal Parenchyma (RP), Renal Blood Flow (RBF), Glomerular Filtration Rate (GFR), Adaptive NLM filtering, Chan-Vese (CV) level sets, K-Means, Dice Coefficient and Jaccardian Index.

DOI: 10.24297/j.cims.2023.4.7

1. Introduction

Identification of fractures or abnormalities from organs may happens by expert or automatically by the processing algorithms may further leads to the treatment. The automatic algorithm extracts the identical features of the defects from the acquired images with the help of pre-defined instructions formed by the experts [1]. The imaging tools producing precise observations on biological functions and make the expert to diagnosis.

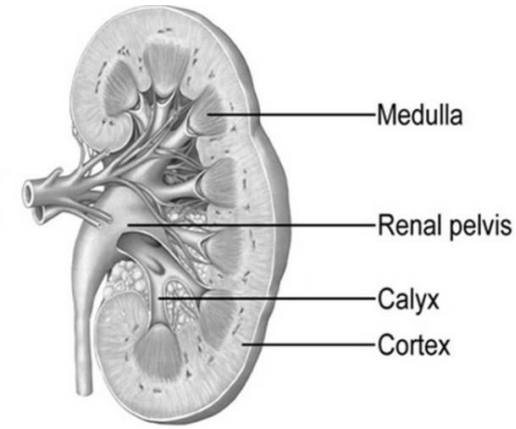

Figure 1 Anatomy of Kidney Structure

As shown in Figure 1 the kidney consists of three main parts such as cortex, medulla and renal pelvis called renal compartments and Cortex and medulla are combined together mentioned as Renal Parenchyma (RP). Size, function and volume of the kidney in terms of Renal Blood Flow (RBF), Glomerular Filtration Rate (GFR) of kidney estimate the type of disease [2].

Kidney Diseases may be Acute, Chronic or Congenital. Acute Kidney Disease (AKD) [3] is malfunctioning of the kidney may develop suddenly due to dehydration, blood loss caused by injury or surgery and the side effects of medicines. It also called Acute Renal failure.

Congenital kidney diseases [4] had developed in individuals caused by abnormalities by birth such as blocking of valves between bladder and ureter allowing infections within the kidney. Polycystic Kidney Disease (PKD), Unilateral Renal Agenesis (URA) and Bilateral Renal Agenesis (BRA) are the common congenital kidney diseases.

Precise measurements of RBF, GFR, total and cortical volume estimates KGR. Similarly, RAS detected by calculating the loss of parenchyma in the stenosed kidneys assessed by measuring total renal and parenchyma volumes in both the kidneys.

Survey on Kidney Diseases: Worldwide, annually there are approximately 750 million people are affected by Kidney diseases. 8–16% of hospital admissions are of AKD [5] and 17 lakhs people died per year from AKI. Nearly, 85 percent of kidneys diseased cases recorded from average income countries, caused to 1.4 million deaths. In 2017, 1.2 million people died because of CKD. Due to lack of treatment, 10% of populations had affected by CKD [6]. Worldwide around 2 million people are under kidney transplantation or dialysis and majority are from the developed Countries [7].In developing countries like in China or in India, kidney disease cases are gradually increasing mostly in elder age and it creates a financial burden.

- The cost of treating chronic kidney disease in the United States had expected to top $48 billion a year. To care for less than 1% of the Medicare population, kidney failure treatment absorbs 6.7 percent of the overall Medicare budget.
- In low- and middle-income countries, 80 percent of the burden is borne by people under the age of 60, and 25 percent by people under the age of 60.
- According to the World Health Organization [8], approximately 58 million people died worldwide in 2005, with 35 million of them dying because of chronic disease.

2. Literature Survey

Segmentation is the major step in assessing Kidney functionality and volume calculation. For kidney volume calculation whole kidney contours should be extracted from the acquired DCE MRI sequences and then each slice volume is calculated. While assessing the kidney functionality, calculating GFR and RBF parameters is important. To get accurate results, an efficient segmentation method is required. Initially kidney contours have extracted from the MRI examinations and then kidney compartments are to be sub segmented.

According to Zöllner et al. [9] kidney image segmentation, methods have classified into three categories. They are

1. Manual Kidney Segmentation
2. Semi automated Kidney Segmentation
3. Automated Kidney Segmentation

In manual kidney segmentation, the operator calculates the dimensions of kidney and volume have estimated by ellipsoid [10] or stereological approach [11]. This segmentation approach is time consuming and the accuracy values of volumes obtained are the operator dependent. They may vary operator to operator depends on the dimensions taken and the process is time consuming.

In Automatic Kidney Segmentation, the operator does not involve in segmentation process. The algorithm designed is automatically detects the kidney structure depends on the predefined shapes of the kidney and then applies the segmentation. This process is time consuming, there is no need to search for the kidneys in the whole image using estimations, and operator interaction is necessary for better results.

In semi automated Kidney segmentation, the operator initially traces the kidney contour roughly and the algorithms accurately defines the kidney contours to segment the whole kidney and then renal compartments were segmented automatically by the proposed algorithm. Based on the segmented portion, the functionally parameters such as GFR, RBF and whole kidney volume and parenchyma volume were calculated.

Many methods were proposed for the segmenting the kidney and parenchyma such as region segmentation, K-means segmentation, active contours and watershed algorithms. Some of these were discussed as a part of the literature survey.

- Xin Yang et al [12] proposed extended *Maximally Stable Extremal Region* (MSTV) based on connected tree components for overall kidney segmentation.Because the segmentation findings are not constrained by shape, it can change its kidney shape for estimating renal disease.
- Timothy L. Kline et al [13] proposed an approach to measure Total Kidney Volume (TVK) through combine deformable and affine registration and segmentation using active contour model to finalize the kidney boarders. Still require quality check by trained image analyst.
- Convolution Neural networks and Active shape models currently become popular in medical image segmentation applications. However, they require enough training data of the objects to cover the physiological variability and depending on synthetic dataset [14].
- For segmenting single structures, Klaus D. Toennies et al [15] devised a model-based adaptive region-growing algorithm.As performance measures, average deviation, Hausdorff distance, number of over-and under-segmented pixels percentages have utilized.
- Using biomedical image processing approaches, Gao yan et al [16] created an automatic system for segmenting kidney on CT images. Then, the position of the kidney had estimated. Kidney region obtained further by using multi-scale morphological operators and region growing algorithm to extract the three kidney regions.
- H. Abdelmunim et al [19] addressed to the problems of DCE-MRI such as spatial resolution during fast scan, motion artifacts due to breathing, non-uniformity of contrast intensity, as it was perfuse into cortex. To improve the results, they took into account both grey level and preceding shape information.
- E.Goceri et al [20] proposed Gaussian Mixture Model (GMM) based kidney segmentation using EM algorithm on MR images.The initial kidney separated into five clusters using an unsupervised clustering method based on a probabilistic model. Each one is fitting a mixture model to a variety of intensities, which made up of many Gaussian distributions. According to intensities, pixels clustered. Then split the kidney using thinning and it used as marker for next slice. The iteration stops if no kidney presented in the slice. The K means partitioning have some miss classification due to inhomogeneity and partial volume effects, which compensated by GMM.

3. Proposed Methodology

This paper presents semi automated kidney image segmentation in which the technician interacts manually in selecting the kidney to be segmented to which the functional or volume parameters are to be calculated using active contours and a simple and fast K-Means segmentation is used to segment the kidney compartments. With the advantages in filtering

process, an adaptive NLM filter is adapted for preprocessing step to reduce the noise present within the MRI images.

The proposed system employs four basic steps.

- The MRI image in DICOM format obtained from image database is converting into jpeg format
- An adaptive NLM filter is used to remove the noise and movement corrections.
- Then active contours are used to segment the whole kidney for its background.
- After getting the image of the kidney of interest, K-Means clustering used to segment the renal cortex, medulla and pelvis.

The segmentation results of the developed system compared with Threshold based FCM with Adaptive NLM preprocessing. The performance has shown in terms of Accuracy, Sensitivity, MCC, Dice coefficient and Jaccardian Index.

3.1. Preprocessing of Kidney MRI Images-Adaptive NLM Filtering

There are many variations in NLM denoising as mentioned in [21] earlier are Fast NLM, block wise optimized NLM, unbiased NLM, Dynamic NLM, Enhanced NLM and Adaptive NLM. Here we have employed NLM algorithm with adaptive search window [22] to improve denoising performance and segmentation accuracy.

In the Non-local means (NLM) algorithm, search window size is a crucial factor. It depends on smoothness or homogeneity of the region as it requires few pixels for denoising and more pixels in a non-smooth or transition region. The algorithm selects the size of search window depends on Gray Level Difference (GLD) image. At higher noise levels, it also retains image information such as edges and texture.

Procedure to implement Adaptive search window with NLM:

1. Initially apply conventional NLM filter on input noisy image.
2. Obtain GLD image for each pixel *i* at *f(k,l)* is $\Delta\hat{f}_i$ using the following equation

$$\Delta\hat{f}_i = |\hat{f}_i - \tilde{f}_i| \quad (1)$$

Where $\hat{f}_i$ is the NLM pre-filtered image of size nxn and

The mean or average values of pixels in the searching window of size nxn is

$$\tilde{f}_i = \frac{1}{nxn}\sum_{k=1}^{n}\sum_{l=1}^{n}\hat{f}(k,l) \quad (2)$$

3. Obtain mean (μ) and standard deviation (σ) from GLD image.
4. Calculate the threshold values T_1 and T_2 using μ and σ as

$$T_1 = \mu \quad (3)$$

$$T_2 = \mu + \alpha\sigma \quad (4)$$

Here α is the controlling parameter, set to 0.4

5. Estimate the optimal search window map S_i^{opt} for each pixel from the GLD image using threshold values T_1 and T_2 as

$$S_i^{opt} = \begin{cases} large & if \quad \Delta\widehat{f_i} < T_1 \\ medium & if \quad T_1 \leq \Delta\widehat{f_i} \leq T_2 \\ small & if \quad \Delta\widehat{f_i} > T_2 \end{cases} \quad (5)$$

6. Finally obtain the denoised image for each pixel using the following equation

$$\hat{f}_{final}(i) = \frac{\sum_{j \epsilon S_i^{opt}} w(i,j) y(j)}{\sum_{j \epsilon S_i^{opt}} w(i,j)} \quad (6)$$

3.2. Segmentation of Whole Kidney

Chan-Vese (CV) algorithm [23] is used to separate the whole kidney from its background and it is a problem to minimize the energy function F(c_1,c_2,C) and solving for C. In levelset formulation, the initial curve drawn by the expert is C which considered as zero level set. In this paper, the curve drawn is a polygon, which is assumed to be the curve for analysis. If Ω represents the whole image region, be the bounded open set of $\mathbb{R}^2$ with $\partial\Omega$ as its boundary. Let $f_0: \bar{\Omega} \rightarrow \mathbb{R}$ is the given image inside the boundary $\partial\Omega$, then the drawn curve is subset of Ω defined by zero levelset of some Lipschitz function Φ: Ω→ $\mathbb{R}$ formulated as

On the Curve,C $= \partial\omega = \{(x,y) \in \Omega: \Phi(x,y) = 0\}$, (7)

Inside the Curve, inside(C) = $\omega = \{(x,y) \in \Omega: \Phi(x,y) > 0\}$, (8)

and

Outside the Curve, Outside(C) =$\bar{\Omega} \backslash \omega = \{(x,y) \in \Omega: \Phi(x,y) < 0\}$, (9)

Here ω is the region inside C and $\bar{\Omega} \backslash \omega$ is the region outside C.

3.3. Segmentation of Renal Compartments

K-Means Clustering is a well-known unsupervised strategy for dividing an unlabeled dataset into related datasets in an iterative fashion, with each data set belonging to only one group with similar qualities. It also called Hard Clustering and useful in clear partitioning of kidney compartments.

The following steps will describe how the K-Means algorithm works:

1. Select the number of clusters, K=4 for background, Renal Pelvis, Medulla and Cortex.
2. Select K centroids at random.
3. Each pixel had assigned to its closest centroid, for K clusters.
4. Calculate the variance and move the centroid of each cluster.
5. Repeat step 3 and reassigning each data point to new cluster centroid.
6. If assignment had not completed go to step-4 and finish the operation

To stop the K-means algorithm, there are essentially three conditions that has to be used:

1. The centroids of freshly generated clusters stay the same.
2. The same cluster of points had maintained.

3. You have achieved the maximum number of iterations.

The method ends if the centroids of freshly created clusters do not change. After several rounds, if all of the clusters have the same centroids, we can conclude that the algorithm is not learning any new patterns and that training stopped. Another sign that the training process stopped is if the points stay in the same cluster after numerous cycles of the algorithm.

4. Experimental Results and Analysis

Datasets

The datasets collected from publicly available TCIA database browsing on the preferences as Imaging Modality: MR, Anatomical site: Kidney and Species: Homo sapiens excluding Phantoms. There are five categories of collections of Kidney volumes in different projections are obtain from different MRI machines such as GE MEDICAL SYSTEMS, SIEMENS, TOSHIBA_MEC and Philips Medical Systems with different subject IDs.

We are mainly concentrate on Axial and coronal projections and selected 32 volumes with sizes 512x512 and 256x256, thicknesses 4mm, 5mm,6mm,7mm, 8mm and corresponding the spacing of 1.5mm,2mm,2.5 mm,3mm,6mm and 8mm respectively.

From each kidney volume, sequence the slice with maximum kidney area had obtained from different series and then converted those into jpeg formate.Totally there are 172 images have extracted manually for segmentation purpose. Each image used in this paper mentioned with its ID, sequence number and slice number. The sequence/series number differentiates the projection series. The image shown in Figure 3(a) extracted for male subject at an age of 41 years using GE MEDICAL SYSTEMS, COR KIDNEY1 PRE sequence with slice number 11 out of 20.

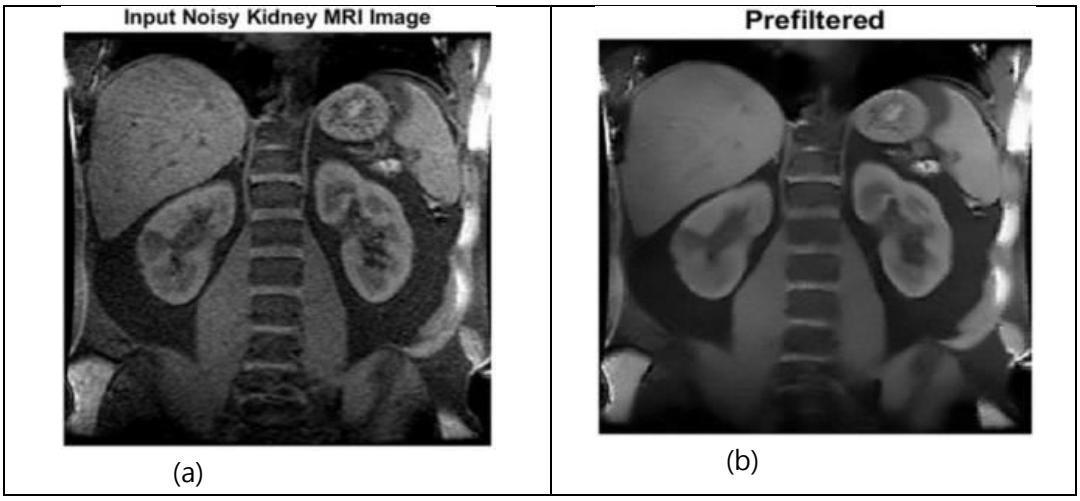

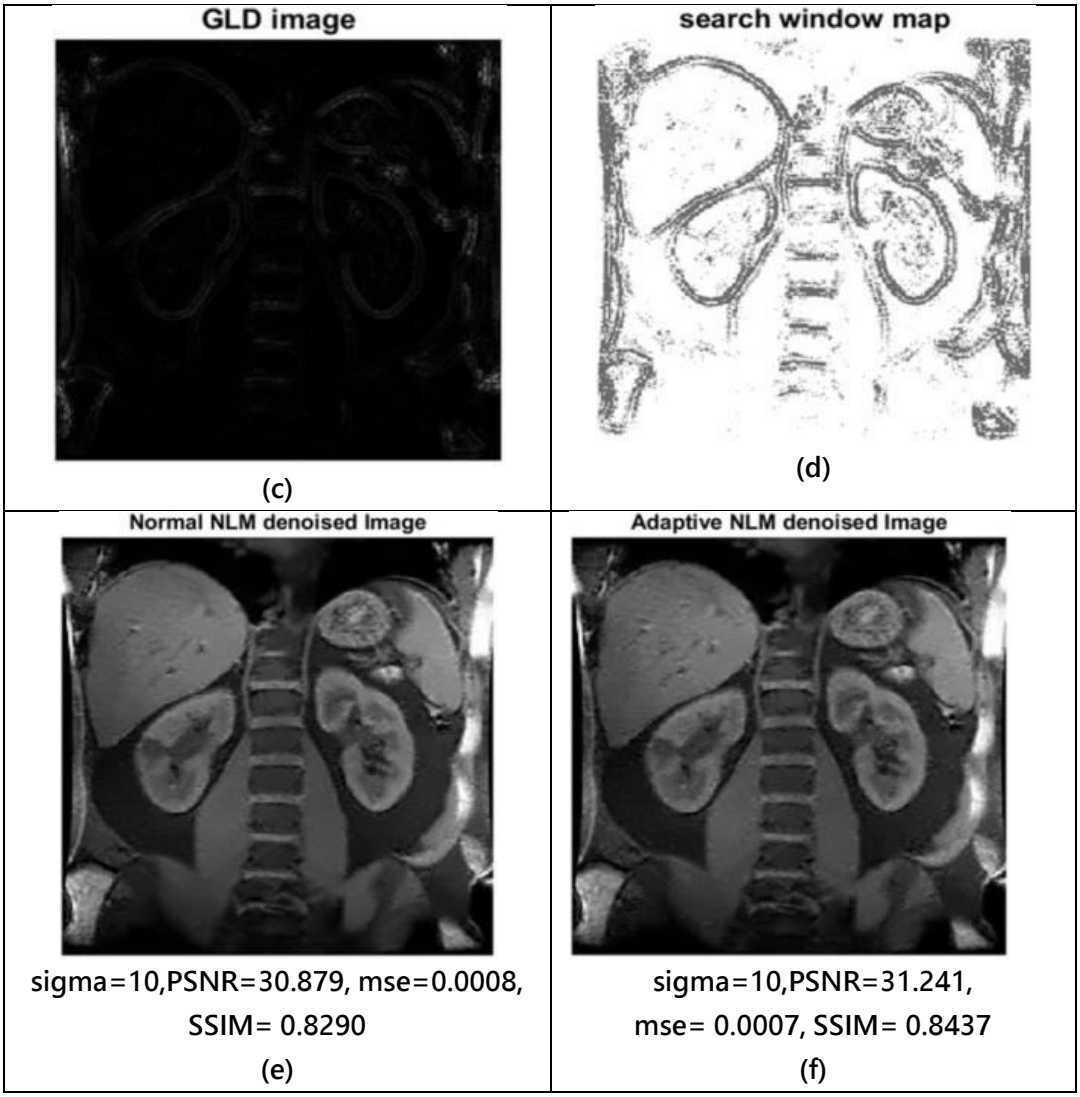

Figure 3. Preprocessing of Kidney MRI Noisy Image. (a) Input Kidney noise MRI Image (b) NLM filtered image (c) Gray Level Difference Image (d) Search window map for GLD Image (e) PSNR,MSE and SSIM of NLM denoised image with sigma=10 (f) PSNR,MSE and SSIM of Adaptive NLM denoised image with sigma=10 .

Table 1 compares the noise characteristics of the traditional NLM algorithm with the adaptive NLM algorithm for various sigma values. In terms of PSNR, MSE, and SSIM, it can be see that the suggested denoising technique outperforms the standard algorithm. Figure 3 depicts a noisy image and the sequence of images according to algorithm as mentioned earlier with a sigma value of 10.

Table 1 Comparing noise characteristics for NLM and Adaptive NLM Filtering

Sigma	NLM Filtering			Adaptive NLM Filtering		
	PSNR	MSE	SSIM	PSNR	MSE	SSIM
10	30.8799	0.0008	0.8290	31.2414	0.0007	0.8437

20	27.7546	0.0017	0.6853	28.2044	0.0015	0.7092
30	25.9103	0.0026	0.5956	26.4226	0.0023	0.6239
40	24.6833	0.0034	0.5436	24.9220	0.0032	0.5572
50	23.7730	0.0042	0.5084	23.6092	0.0044	0.4969

(a). After Preprocessing shown in Figure (3), the whole kidney is separated from its background using Active contour Levelset Segmentation.

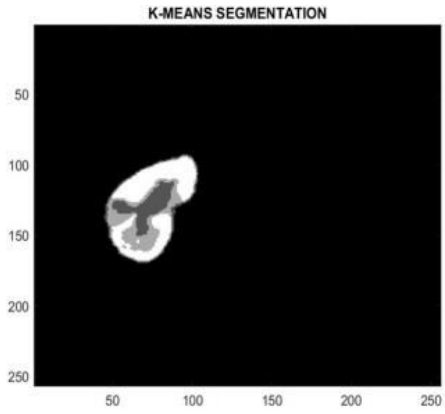

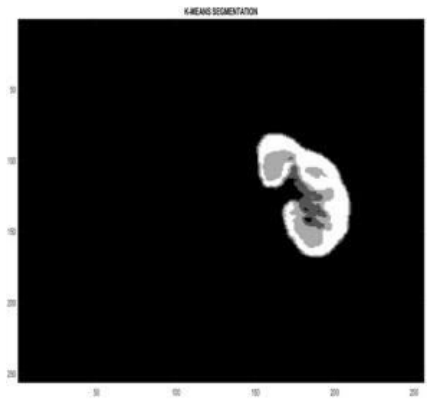

(b). Differentiating Medulla, Pelvis and Cortex using gray levels of each kidney using K-means Clustering Algorithm.

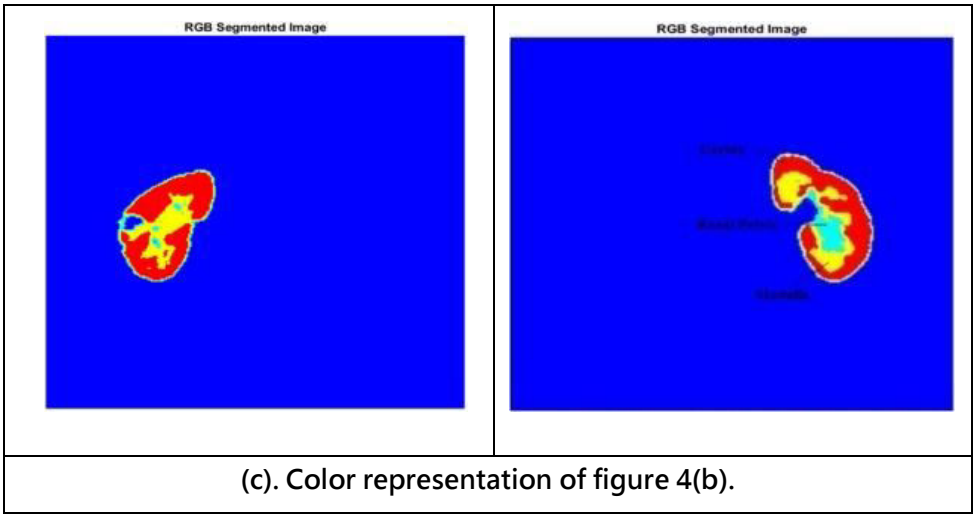

(c). Color representation of figure 4(b).

Figure 4. Segmentation of Kidney MRI Image. (a) Separating kidney from its background (Blue) (b) gray level representation (c) Color differentiation of Kidney Compartments, Renal Pelvis(Aqua), Cortex(Red) and Medulla(Yellow) Left side columns shows Left Kidney and Right side columns shows Right Kidney separation

After preprocessing, the two kidneys had separated from their background using Active contour levelset segmentation. Since the proposed system is semi automatic, the user manually drawn the boundary mask as a polygon and the level sets proceeds to the boundaries iteratively until the whole kidney boundaries extracted. Then a pixel wise product multiplication has done to extract the whole kidney. To separate the two kidney images an algorithm applied twice.

The Kidney image had further partitioned by K-Means segmentation algorithm. Here K-Means algorithm had used because it is a hard clustering technique and we need to group the pixels in four groups. The Kidney itself is having three compartments such as Cortex, Medulla and Pelvis. The pixels within the kidney may essentially belong to any one of these three and the all block pixels of back background together as one group. The algorithm had given result in portioning kidney compartments and represented by different colors as shown in Figure 4.

The performance of segmentation algorithm measured in performance metrics [24] such as Accuracy, Sensitivity, MCC, Dice Coefficient and Jaccard Index as defined below and corresponding values shown in Table2.The graph shown in Figure 5 and Figure 6 represents that the accuracy and Jaccardian Index are higher for K-Means and Threshold based FCM Algorithm [25]. It shows that we are getting an average of 99.68 percent Accuracy and a sensitivity of nearly 1, MCC of 0.9462 and very good Dice and Jaccardian Coefficients of 0.9462 and 0.8992 respectively.

$$Accuracy = \frac{TP+TN}{FN+FP+TP+TN} \quad (29)$$

$$Sensitivity = \frac{TP}{FN+TP} \quad (30)$$

$$MCC = \frac{(TP*TN)-(FP*FN)}{\sqrt{(TP+FP)*(TP+FN)*(TN+FP)*(TN+FN)}} \quad (31)$$

$$DICE\ Coefficient = \frac{2*TP}{2*TP+FP+FN} \quad (32)$$

$$Jaccard\ Index = \frac{DICE\ Coefficient}{2-DICE\ Coefficient} \quad (33)$$

Table 2. Performance Metrics (Accuracy, Sensitivity, MCC, Dice Coefficient, Jaccard Index) at Sigma=10

Dataset		K-means Clustering					Threshold based FCM				
		Accuracy	Sensitivity	MCC	Dice	Jaccard	Accuracy	Sensitivity	MCC	Dice	Jaccard
4807-11-11-WOC.jpg	left	0.9981	0.9979	0.9777	0.9784	0.9578	0.9822	0.5732	0.7502	0.7287	0.5732
	Right	0.9967	0.9997	0.9649	0.9660	0.9343	0.9793	0.5411	0.7278	0.7022	0.5411
5200-12-57-WC.jpg	left	0.9974	1	0.9689	0.9698	0.9413	0.9833	0.4786	0.6859	0.6474	0.4786
	Right	0.9962	1	0.9575	0.9586	0.9204	0.9894	0.6190	0.7825	0.7646	0.6190
4762-9-33-WC.jpg	left	0.9984	0.9998	0.9547	0.9545	0.9129	0.9942	0.6529	0.8056	0.7900	0.6529
	Right	0.9978	1	0.9342	0.9332	0.8748	0.9916	0.4630	0.6776	0.6329	0.4630
5006-11-34-WC.jpg	left	0.9947	0.9983	0.8968	0.8944	0.8090	0.9883	0.4782	0.6874	0.6470	0.4782
	Right	0.9953	0.9985	0.9157	0.9147	0.8428	0.9884	0.5423	0.7321	0.7032	0.5423
	Average	**0.9968**	**0.9993**	**0.9463**	**0.9462**	**0.8992**	**0.9870**	**0.5435**	**0.7311**	**0.7020**	**0.5435**

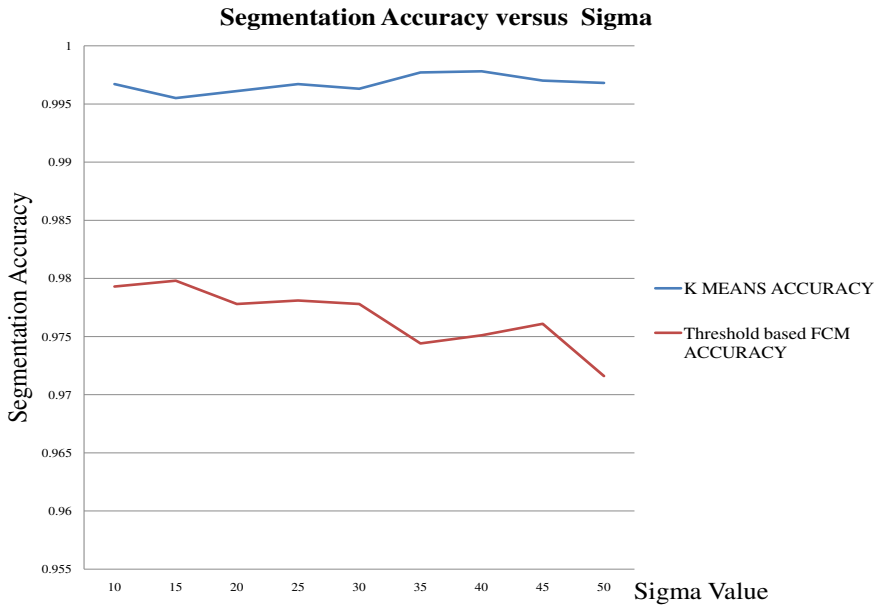

Figure 5. Segmentation Accuracy Comparison for both K-Means and Threshold based FCM Algorithms

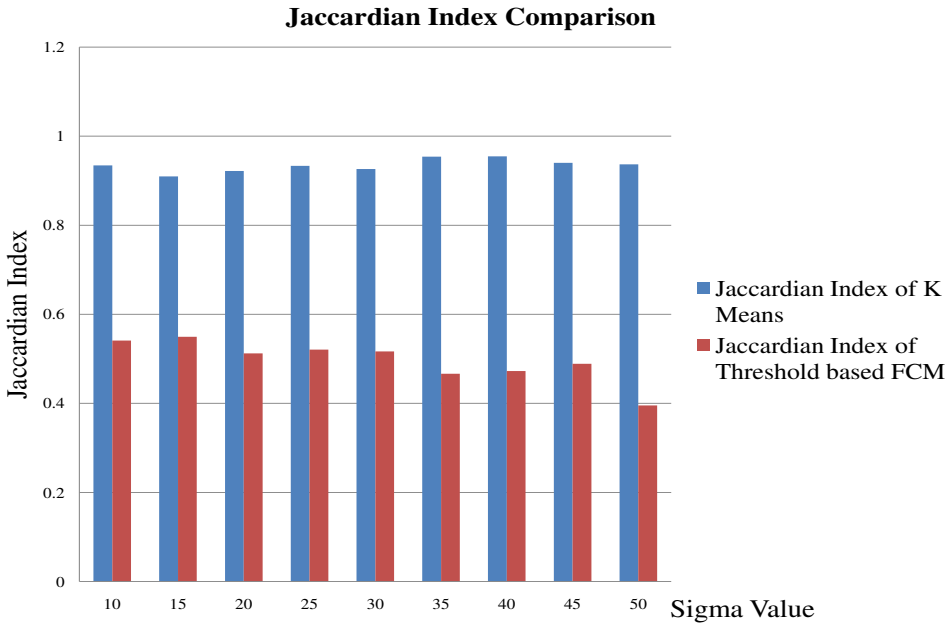

Figure 6. Jaccardian Index Comparison for both K-Means and Threshold based FCM Algorithms

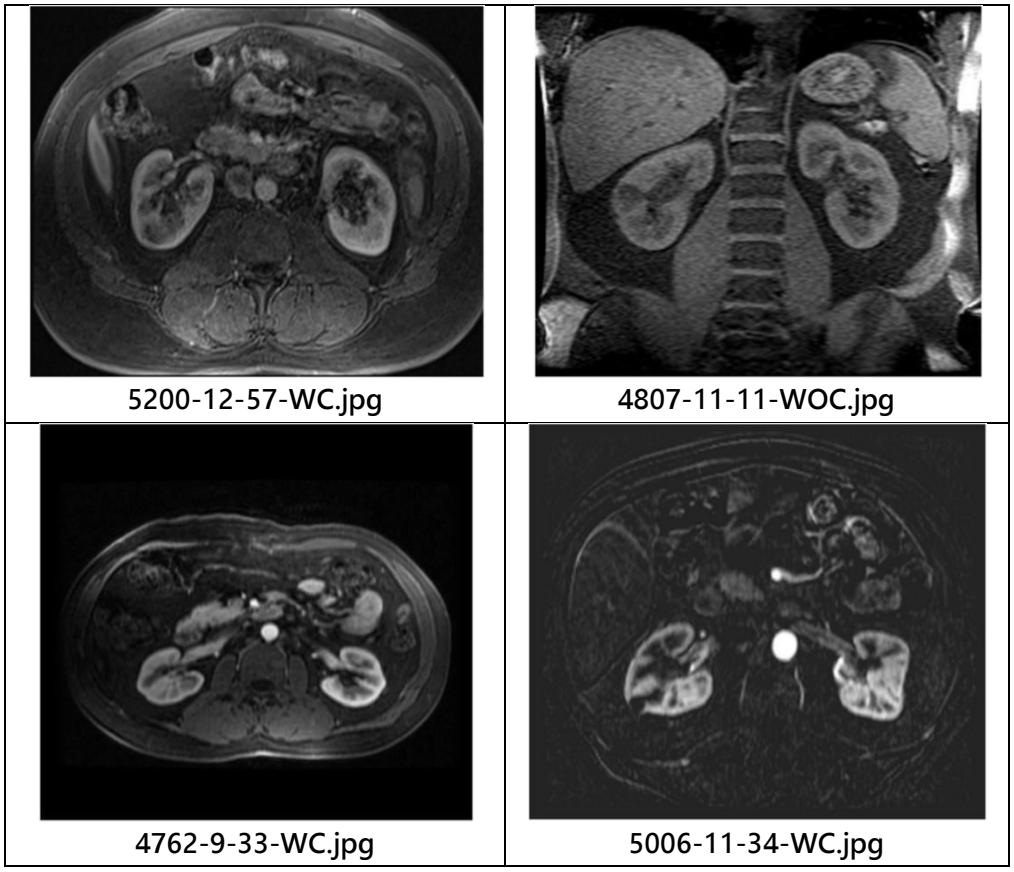

Figure 7. Dataset used for getting Performance Metrics

5. Conclusion

This paper presents semi automated kidney image segmentation in which the technician interacts manually in selecting the kidney to be segmented to which the functional or volume parameters are to be calculated using active contours and a simple and fast K-Means segmentation is used to segment the kidney compartments. With the advantages in filtering process, an adaptive NLM filter is adapted for preprocessing step to reduce the noise present within the MRI images.

The Chan-Vese algorithm is a very powerful algorithm that works well even with images that are difficult to segment with gradient-based methods or thresholding. The datasets used for evaluation of segmentation performance shown in Figure 7. The segmentation results of the developed system had compared with threshold based FCM with same denoising algorithm and whole kidney segmentation. The performance had shown in terms of Accuracy, Sensitivity, MCC, Dice and Jaccard coefficients.

References

1. Bowling, C.B., Hall, R.K. (2021). Kidney Disease. In: Lee, A.G., Potter, J.F., Harper, G.M. (eds) Geriatrics for Specialists. Springer, Cham. https://doi.org/10.1007/978-3-030-76271-1_23
2. Sharma N, Aggarwal LM. Automated medical image segmentation techniques. J Med Phys. 2010;35(1):3-14. doi:10.4103/0971-6203.58777
3. Julka, R., Reddy, A. (2013). Acute Kidney Injury. In: Wong, C., Hamlin, N. (eds) The Perioperative Medicine Consult Handbook. Springer, New York, NY. https://doi.org/10.1007/978-1-4614-3220-3_19
4. Grünfeld, JP. Congenital/inherited kidney diseases: how to identify them early and how to manage them. *Clin Exp Nephrol* **9,** 192–194 (2005). https://doi.org/10.1007/s10157-005-0352-0
5. Crews DC, Bello AK, Saadi G. Burden, access, and disparities in kidney disease. Clin Nephrol. 2019 Mar;91(3):129-137. doi: 10.5414/CN91WKDEDI. PMID: 30704553.
6. World Kidney Day: Chronic Kidney Disease.2015: http://www.worldkidneyday.org/faqs/chronic-kidney-disease/
7. Couser WG, Remuzzi G, Mendis S, Tonelli M. The contribution of chronic kidney disease to the global burden of major noncommunicable diseases. Kidney Int. Dec 2011;80(12):1258-1270.
8. Christian Delles, Raymond Vanholder; Chronic kidney disease. Clin Sci (Lond) 1 February 2017; 131 (3): 225–226. doi: https://doi.org/10.1042/CS20160624.
9. Zöllner FG, Svarstad E, Munthe-Kaas AZ, Schad LR, Lundervold A, Rørvik J. Assessment of kidney volumes from MRI: acquisition and segmentation techniques. AJR Am J Roentgenol. 2012 Nov;199(5): 1060-9. doi: 10.2214/AJR.12.8657. PMID: 23096180.
10. Irazabal MV, Rangel LJ, Bergstralh EJ, Osborn SL, Harmon AJ, Sundsbak JL, et al: Imaging classification of autosomal dominant polycystic kidney disease: a simple model for selecting patients for clinical trials. J Am Soc Nephrol 2015; 26: 160–172.
11. Emilie Cornec-Le Gall, Ahsan Alam, Ronald D Perrone, Autosomal dominant polycystic kidney disease, The Lancet, Volume 393, Issue 10174, 2019, Pages 919-935, ISSN 0140-6736, https://doi.org/10.1016/S0140-6736(18)32782-X.
12. Yang X, Le Minh H, Tim Cheng KT, Sung KH, Liu W. Renal compartment segmentation in DCE-MRI images. Med Image Anal. 2016 Aug;32:269-80. doi: 10.1016/j. media. 2016.05.006. Epub 2016 May 16. PMID: 27236222.
13. Kline TL, Korfiatis P, Edwards ME, Warner JD, Irazabal MV, King BF, Torres VE, Erickson BJ. Automatic total kidney volume measurement on follow-up magnetic resonance images to facilitate monitoring of autosomal dominant polycystic kidney disease progression. Nephrol Dial Transplant. 2016 Feb;31(2):241-8. doi: 10.1093/ndt/gfv314. Epub 2015 Aug 31. PMID: 26330562; PMCID: PMC4725388.
14. Milletari, F., Navab, N., and Ahmadi, S.-A. (2016). V-Net: Fully Convolutional Neural Networks for Volumetric Medical Image Segmentation. In 2016 Fourth International Conference on 3D Vision (3DV), pages 565–571. IEEE.

15. D. Q. Zeebaree, H. Haron, A. M. Abdulazeez and D. A. Zebari, "Machine learning and Region Growing for Breast Cancer Segmentation," 2019 International Conference on Advanced Science and Engineering (ICOASE), 2019, pp. 88-93, doi: 10.1109/ICOASE.2019.8723832.
16. E. Gibson et al., "Automatic Multi-Organ Segmentation on Abdominal CT With Dense V-Networks," in IEEE Transactions on Medical Imaging, vol. 37, no. 8, pp. 1822-1834, Aug. 2018, doi: 10.1109/TMI.2018.2806309.
17. M. El-Melegy, R. A. El-karim, A. El-Baz and M. A. El-Ghar, "Fuzzy Membership-Driven Level Set for Automatic Kidney Segmentation from DCE-MRI," 2018 IEEE International Conference on Fuzzy Systems (FUZZ-IEEE), 2018, pp. 1-8, doi: 10.1109/FUZZ-IEEE.2018.8491552.
18. Goceri E. (2011) Automatic Kidney Segmentation Using Gaussian Mixture Model on MRI Sequences. In: Wan X. (eds) Electrical Power Systems and Computers. Lecture Notes in Electrical Engineering, vol 99. Springer, Berlin, Heidelberg. https://doi.org/10.1007/978-3-642-21747-0_4
19. J. Mohan, V. Krishnaveni, Yanhui Guo, A survey on the magnetic resonance image denoising methods, Biomedical Signal Processing and Control, Volume 9, 2014, Pages 56-69, ISSN 1746-8094, https://doi.org/10.1016/j.bspc.2013.10.007.
20. R. Verma and R. Pandey, "Non local means algorithm with adaptive isotropic search window size for image denoising," 2015 Annual IEEE India Conference (INDICON), 2015, pp. 1-5, doi: 10.1109/INDICON.2015.7443193.
21. M. Zawish, A. A. Siyal, K. Ahmed, A. Khalil and S. Memon, "Brain Tumor Segmentation in MRI images using Chan-Vese Technique in MATLAB," 2018 International Conference on Computing, Electronic and Electrical Engineering (ICE Cube), 2018, pp. 1-6, doi: 10.1109/ICECUBE.2018.8610987.
22. Kumari, L.K., Jagadesh, B.N. Classification of mammograms using adaptive binary TLBO with ensemble classifier for early detection of breast cancer. *Int. j. inf. tecnol.* (2022). https://doi.org/10.1007/s41870-022-00998-7
23. M. Khandelwal, S. Shirsagar and P. Rawat, "MRI image segmentation using thresholding with 3-class C-means clustering," 2018 2nd International Conference on Inventive Systems and Control (ICISC), 2018, pp. 1369-1373, doi: 10.1109/ICISC.2018.8399032.